JOURNAL OF APPLIED ELECTROCHEMISTRY 15 (1985) 379–386

Sodium activity determinations in molten 99.5% aluminium using solid electrolytes

P. C. YAO*, D. J. FRAY

Department of Metallurgy and Materials Science, University of Cambridge, Pembroke Street, Cambridge CB2 3QZ, England

Received 16 March 1984; revised 23 July 1984

The thermodynamics of the Na–Al (99.5%) system has been investigated over a range of temperatures. Measurements were made using Nasicon ($Na_3Zr_2Si_2PO_{12}$) and sodium β-alumina with $Na_{0.75}CoO_2$ as the reference material. Near to the melting point there is a strong dependence of the activity coefficient on the sodium concentration whereas, at higher temperatures, Henry's Law is obeyed and the activity coefficient agrees with other determinations.

1. Introduction

Aluminium is produced commerically by the electrolysis of alumina dissolved in molten cryolite and it is observed that codeposition of sodium occurs with the aluminium at the cathode. During subsequent processing much of the sodium is lost by evaporation and oxidation. If, however, the aluminium is to be used for the production of aluminium–magnesium alloys it is imperative that the sodium content is reduced to below 2 ppm. In another context, aluminium–silicon alloys, sodium is added to modify the eutectic structure to give a high strength alloy. As mentioned above, sodium is a particularly volatile element, and this leads to problems with sampling and to differences in the quoted analytical results [1–3]. It is, therefore, important to have a thorough understanding of the thermodynamics of the aluminium–sodium system [4, 5] and to develop a device for the on-line monitoring of sodium [6, 7]. Brisley and Fray [7] showed, that in agreement with the work of Dewing [5], the activity of sodium in superpurity aluminium obeys Henry's law. However, at 998 K, 0.05% of impurity made the activity coefficient strongly dependent on the sodium content. It is surprising that such a dramatic change should occur for such a small addition and this needs further investigation.

All other electrochemical determinations of the sodium activity have been made using sodium β-alumina as the solid electrolyte. Since the discovery of the high sodium mobility in sodium β-alumina other sodium solid electrolytes have been developed. Hong [8] and Goodenough [9] synthesized solid solutions of $NaZr_2(PO_4)_3$ and $Na_4Zr_2(SiO_4)_3$. It was found that $Na_3Zr_2Si_2PO_{12}$ had a sodium ion conductivity which exceeded 0.3 ohm^{-1} cm^{-1} at 573 K which is equal to the conductivity of β″-alumina at this temperature. In addition, the material has a somewhat higher activation energy, 0.24 eV as opposed to 0.18 eV in β″-alumina, which makes $Na_3Zr_2Si_2PO_{12}$ a superior sodium ion conductor above 573 K. It seemed appropriate to investigate this material as an electrolyte for the determination of the sodium activity in molten metals.

The reference material should contain sodium at a fixed activity and this has usually been arranged by using a mixture of α + β-alumina [6, 7] and fixing the oxygen partial pressure by either exposing the reference to the air or by a mixture of copper–copper oxide or another metal and its oxide. A disadvantage of this system is that the reference material is an ionic rather than an electronic conductor. It is anticipated that a better probe performance would be attained with an electronic conductor. Solid solution electrodes have been

*Present address: The Chung Shan Institute of Science and Technology, Taiwan, Republic of China.

0021–891X/85 $03.00 + .12.

successfully used in secondary batteries and the electrodes consist of a non-stoichiometric compound which can function as a host lattice for the incorporation of many elements such as hydrogen, copper, lithium and sodium. Steele [10] has outlined the properties of solid solution electrodes as follows:

1. Large range of homogeneity.
2. Partial molar free energy of the electroactive species should be relatively constant over a wide range of composition.
3. Good electronic conductor.
4. Rapid chemical diffusion of the electroactive species within the non-stoichiometric electrode.
5. No significant interaction with the electrolyte phase.

After a search of possible systems, it was decided that at 1073 K Na_xCoO_2 [11] ($x \leqslant 1$) offered the best prospects. Under an oxygen pressure of 1 bar and over the temperature range 733–1073 K, four phases have been observed $0.55 \leqslant x \leqslant 0.6$ (P'3); $0.64 \leqslant x \leqslant 0.74$ (P2); $x = 0.77$ (O'3) and $x = 1$ (O3). In all the structures the lattice is built up by sheets of edge sharing CoO_6 octahedra between which the alkali ions are inserted with a trigonal prismatic (P) or octahedral (O) arrangement. Previous work on isostructural phases has shown that there is high ionic mobility in this type of material especially when the alkali ions are intercalated in the trigonal-prismatic environment. It was, therefore, decided to investigate the use of a solid solution reference electrode in the system Na_xCoO_2 ($x \leqslant 1$).

2. Experimental procedure

2.1. *Preparation of* $Na_{1+x}Zr_2Si_xP_{3-x}O_{12}$

The starting materials were anhydrous Na_2CO_3, ZrO_2, precipitated SiO_2 and $NH_4H_2PO_4$. The chemicals were weighed out in the necessary ratios and mixed for 16 h in an alumina ball mill with cylindrical alumina balls using absolute alcohol as an aid to mixing. After drying, the powder was preheated at 573 K for 4 h to decompose the ammonium dihydrogen phosphate and then calcined at 1223 K for 16 h in air in an alumina crucible. The product was ground for 5 days, using the ball mill with absolute alcohol, and pan dried. The calcined and ground powder was cold pressed into rods or tubes by isostatically pressing under 36 kN cm^{-2} without using a binder. To prepare the tubes a mandrel machined from stainless steel was used with a slight taper to facilitate the removal of the pressed tube. The mandrel plus powder was enclosed in a PVC tube of diameter 20 mm and wall thickness 5 mm and the ends closed with rubber bungs. This was then placed in a hydrostatic press to form the tube. The cold formed specimens were sintered in air at about 1473 K for several hours.

2.2. *Preparation of* Na_xCoO_2

The starting materials for synthesizing Na_xCoO_2 were Na_2O_2 and Co_3O_4 which were weighed out in the necessary stoichiometric ratios using the following postulated reactions:

$$Co_3O_4 + (3x/2)Na_2O_2 \rightarrow 3\,Na_xCoO_2 + [(3x/2) - 1]\,O_2 \quad \text{for } x \geqslant 2/3$$

and

$$Co_3O_4 + (3x/2)Na_2O_2 + [1 - (3x/2)]\,O_2 \rightarrow 3\,Na_xCoO_2 \quad \text{for } x \leqslant 2/3$$

Samples of nominal compositions Na_xCoO_2 with $x = 0.6, 0.75, 0.825, 0.9$ and 1.0 were prepared by heating Na_2O_2 and Co_3O_4 mixtures in air at 1173 K for several hours followed by grinding to a fine powder using an agate mortar.

2.3. *X-ray powder analysis*

Powder diffraction patterns of specimens were taken using a Phillips Model 1730 vertical diffractometer in order to assess the phases present within the sintered articles and to determine the lattice parameters of the synthesized polycrystals. The lattice parameters were determined using a least squares analysis and a program developed by G. M. Sheldrick of the Department of Chemistry, University of Cambridge following the method of De Wolff.

2.4. *Scanning electron microscopy*

An ISI-100A scanning electron microscope was

used for the examination of the fracture surfaces of the synthesized solid electrolyte specimens. Fracture specimens were prepared by fracturing the electrolytes in a mortar. The fractured samples were then glued to aluminium stubs with gold sputtered onto the surface and colloidal graphite applied to the edges in order to improve the electrical conduction. All images were taken at 40 kV using a secondary emission detector as the sensor.

2.5. *Determination of sodium activity in reference material* $Na_{0.75}CoO_2$

The following electrochemical cell was set up:

$$\text{stainless steel}\text{–}Na_{(l)}|Na^+ \text{ conductor}|Na_xCoO_2$$

$$(x = 0.75)\text{–stainless steel}$$

The Na^+ conductor was either $Na_3Zr_2Si_2PO_{12}$ or Na β-alumina. The sodium, together with a stainless steel lead, was placed inside the electrolyte tube. The reference material, sodium cobalt bronze $Na_{0.75}CoO_2$ powder, was compressed along with a stainless steel plate into a zirconium oxide crucible and assembled according to Fig. 1. Dry purified argon was introduced and the cell was brought to the starting temperature. When the temperature had stabilized potential measurements were recorded via a Keithley 610C electrometer with a dual chart recorder to confirm the stability of the readings.

2.6 *Determination of sodium activity in molten aluminium*

The schematic diagram of the apparatus is shown in Fig. 2. Well sintered $Na_3Zr_2Si_2PO_{12}$ polycrystalline tubes were used as the electrolyte and $Na_{0.75}CoO_2$ as the reference, which was packed into the electrolyte tube with a stainless steel load. The probes were carefully preheated, prior to immersion in the molten aluminium, to prevent failure from thermal shock. Samples were taken from the melt with a small steel ladle which was coated periodically with an alumina based cement to prevent aluminium attack. Pencil shaped samples were cast in a two-pin mould and sent to Alcan International Ltd, Arvida, Quebec for analysis by spark emission spectroscopy.

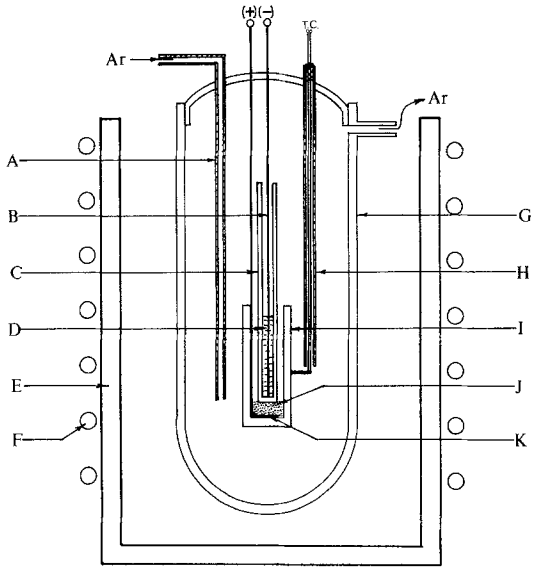

Fig. 1. Cell for the measurement of the sodium activity in the reference material: A, α-alumina tube; B, stainless steel lead; C, Na:β-alumina; D, sodium, E, furnace inner chamber; F, heating element; G, α-alumina tube; H, thermocouple, I, ZrO_2 crucible; J, Na_xCoO_2 ($x = 0.75$); K, stainless steel plate and lead.

3. Results

3.1. *Scanning electron microscopy*

Fig. 3 shows a SEM micrograph of well sintered Nasicon, whereas Fig. 4 shows the fracture surfaces of Nasicon which has been exposed to molten aluminium showing minimal attack.

3.2. *X-ray measurements*

3.2.1. $Na_{1+x}Zr_2Si_xP_{3-x}O_{12}$. X-ray patterns taken at room temperature for $x = 2.0$, 2.2, 2.3 and 2.4 were fitted to a monoclinic and rhombohedral unit cell. For the rhombohedral phase only single reflection should be observed, while for the monoclinic phase the reduction in symmetry leads to a splitting of the X-ray reflections. A slight splitting of diffraction peaks was observed for the $x = 2.0$ and 2.2 compositions. For $x = 2.0$, 2.2 and 2.4, a small amount of ZrO_2 was also detected. The electrolyte with composition $x = 2.3$ seems to be a mixture of rhombohedral and monoclinic phases. Examination of the structure after the electrolyte had been immersed in molten aluminium showed an identi-

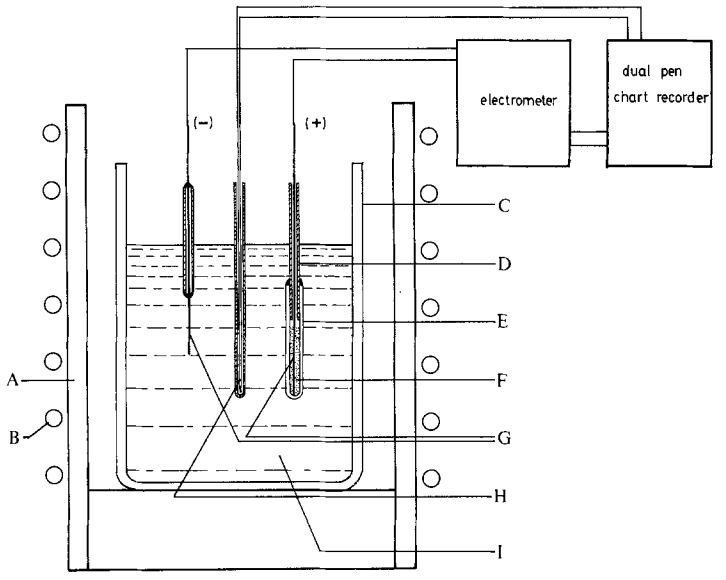

Fig. 2. Schematic diagram of probe construction and apparatus used for the measurement of the activity of sodium in molten aluminium: A, furnace inner chamber; B, heating element; C, crucible; D, α-alumina protection tube; E, solid electrolyte: $Na_3Zr_2Si_2PO_{12}$; F. Reference material: $Na_{0.75}CoO_2$; G, Stainless steel lead; H, thermocouple; I, aluminium melt.

cal diffraction pattern as freshly synthesized Nasicon.

3.2.2. Na_xCoO_2. Room temperature X-ray powder diffraction patterns were made on the system Na_xCoO_2 with $x = 0.6, 0.75, 0.825, 0.9$ and 1.0. The γ phase was found to exist between $x = 0.6$ and 0.75. Diffractrograms of air synthesized $Na_{0.825}CoO_2$, $Na_{0.9}CoO_2$ and $NaCoO_2$ show that there are at least two phases that exist which do not appear in the published phase diagram for this system [11, 12]. This may be due to the different oxygen partial pressure used in these experiments.

3.3. *Activity of sodium in the reference material*

The e.m.f.'s as a function of temperature are shown in Fig. 5 for the cell

$$\text{stainless steel–Na}\,|\,\text{Na}^+\text{ electrolyte}\,|$$

$$(Na_{0.75}CoO_2)_{air}\text{–stainless steel}$$

where the electrolyte was either Nasicon or sodium β-alumina. The data is given by

$$E_{cell} = -9.257 \times 10^{-4}\,T(K) + 2.732\,V \quad (1)$$

When the potential is extrapolated back to 298 K, it gives a value close to that observed by Delmas *et al.* [12].

Fig. 3. Fracture surface of Nasicon sintered at 1433 K × 0.9 K.

Fig. 4. Fracture surface of Nasicon which had been in contact with molten aluminium at 1073 K for 24 h. × 0.9 K.

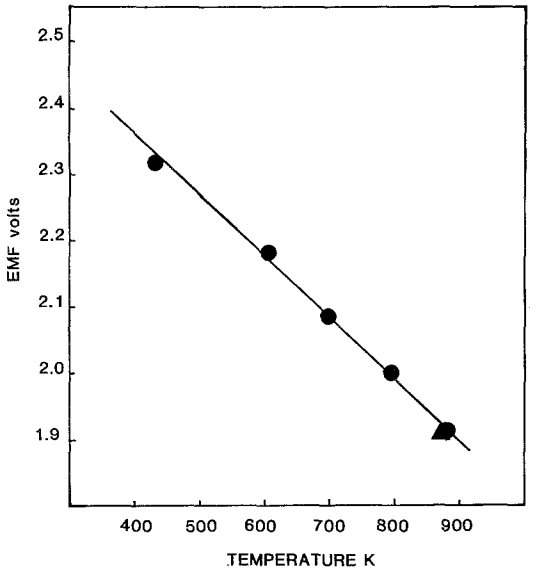

Fig. 5. Plot of potential versus temperature for the cell, stainless steel–Na | Na^+ electrolyte | $Na_{0.77}CoO_2$–stainless steel. • Na β-alumina electrolyte, ▲ Nasicon electrolyte.

3.4. *E.m.f measurements in molten aluminium*

Sodium probes with the following cell construction

stainless steel–$Na_{(Al)}$|Nasicon|

Na_xCoO_2–stainless steel

were used to measure the sodium activity in molten aluminium as a function of temperature. Measurements were made in molten aluminium (99.5% purity) with sodium contents between 1 and 25 ppm over the temperature range 998–1093 K.

The effect of constant current (0.25 mA cm^{-2}) charging and discharging (Fig. 6) of the cell shows that $Na_{0.75}CoO_2$ is a good solid solution reference material as the e.m.f declined to its original value over 3–4 h after titration and, therefore, after preliminary measurements, this compound was used as the reference material. The e.m.f generated by the probe in aluminium with a particular sodium content was compared with the sodium content as determined by analysis. Fig. 7–9 show the e.m.f as a function of composition at 1023, 1068 and 1098 K.

4. Discussion of results

4.1. *Preparation of electrolyte, identification and chemical stability*

A systematic X-ray powder diffraction survey of the phases observed in the $Na_{1+x}Zr_2Si_xP_{3-x}O_{12}$ system with $x = 2.0$, 2.2, 2.3 and 2.4, show that a phase transformation exists between $x = 2.2$ and 2.4, which is in agreement with the work of Hong [8].

The splitting of diffraction peaks is a useful criterion to identify the ambiguity between rhombohedral and monoclinic phases as for the rhombohedral phase only single reflections should be observed, while for the monoclinic distorted phase, the reduction in symmetry leads to a splitting of the X-ray reflections. As expected, the sodium zirconium silicophosphates prepared by solid state reactions using Na_2CO_3, ZrO_2, SiO_2 and NH_4H_2

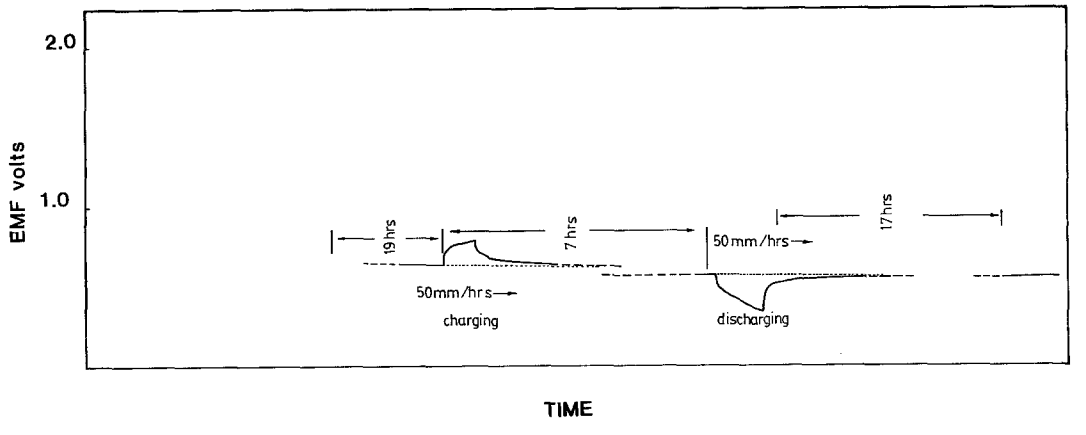

Fig. 6. Typical response of Nasicon probe after electrochemical titration.

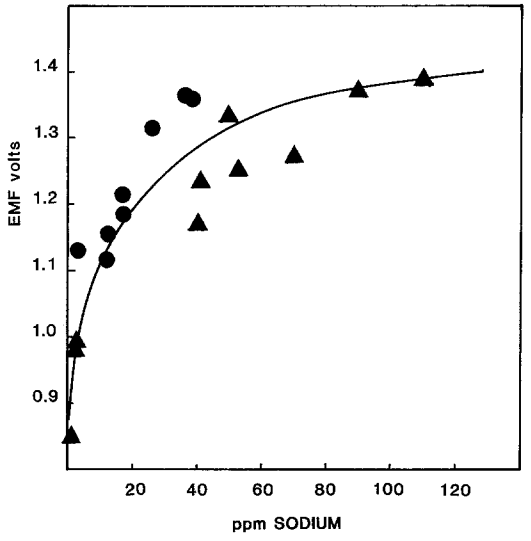

Fig. 7. Plot of potential versus sodium content of aluminium at 1023 K. • This work, ▲ R. J. Brisley [16].

PO_4, are extremely difficult to obtain as a single phase as usually some ZrO_2 remains unreacted with perhaps the formation of a glassy silicate phase. Small amounts of unreacted ZrO_2 were found in this investigation. The electrolyte with composition of $x = 2.3$ seems to be a mixture of rhombohedral and monoclinic distorted phases which may possibly be the reason that $Na_{3.3}Zr_2Si_{2.3}O_{0.7}O_{12}$ electrolyte is hard to sinter and always shows loose bonding between grains. During the determination of activity of sodium in the reference material, the structure of the Nasicon remained the same but new unknown phases were observed indicating some attack by the liquid sodium. After immersion in the molten aluminium, there was a surface layer of discoloration but there was no detectable change in the crystal structure.

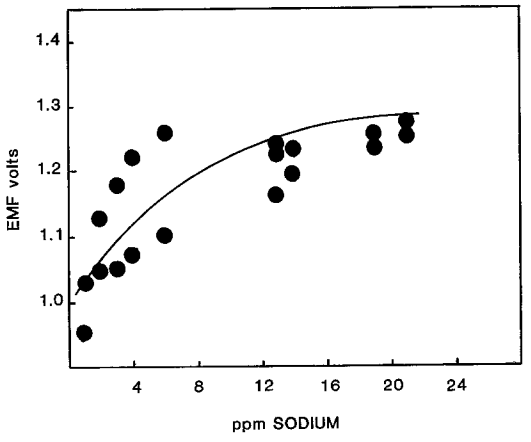

Fig. 8. Plot of potential versus sodium content of Aluminium at 1068 K.

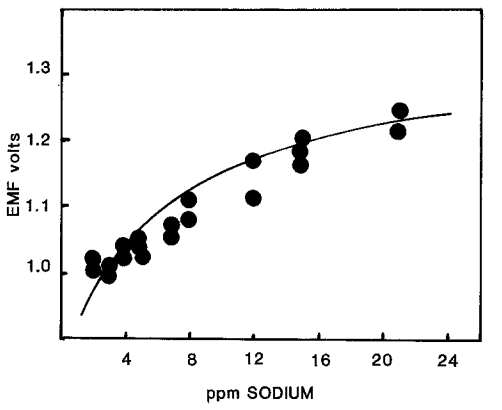

Fig. 9. Plot of potential versus sodium content of aluminium at 1098 K.

4.2. *Determination of activity in sodium in* $Na_{0.75}CoO_2$

From the e.m.f versus temperature plot, the activity of sodium in $Na_{0.75}CoO_2$, exposed to air can be calculated and this is given in Table 1. Both electrolytes were used in these measurements giving identical results.

4.3. *Determination of activity of sodium in 99.5% aluminium*

The activity of sodium in aluminium has been determined independently by Mitchell [4], Dewing [5] and Brisley and Fray [7] using conventional

Table 1. Activity of sodium, relative to pure liquid sodium, in $Na_{0.75}CoO_2$

Temperature (K)	a_{Na}
473	3.08×10^{-25}
573	4.34×10^{-20}
673	1.44×10^{-16}
773	7.24×10^{-14}
873	8.20×10^{-12}

Table 2. Activity coefficient of sodium in Al(99.5%) at 1023 K

ppm	$E_{(V)}$	a_{Na}	γ_{Na} This work	γ_{Na} Brisley and Fray [7] (99.4% Al, 998 K)	γ_{Na} Mitchell and Samis [4] (999 K)	γ_{Na} Brisley and Fray [7] (99.99% Al, 998 K)	γ_{Na} Dewing [5] (99.99% Al)
1	0.85	2.5×10^{-5}	21	17	31	222	385
5	1.05	2.4×10^{-4}	42	25	35	311	385
10	1.15	7.52×10^{-4}	64	25	47	287	385
20	1.20	1.32×10^{-3}	53	54	57	312	385
50	1.325	5.41×10^{-3}	92	86	250	385	385
70	1.36	8.14×10^{-3}	99	137	–	–	385
100	1.385	1.08×10^{-2}	92	110	–	–	385

gas transference techniques, a quenching method and an e.m.f. method using sodium β-alumina, respectively. As can be seen from the Tables, the data of Dewing and Mitchell did not agree, while the work of Brisley agreed with the results of Dewing and for high purity aluminium Henry's law is obeyed. For 99.5% aluminium, it was found that the activity coefficient was strongly dependent on the sodium content. Comparison of the results at 1023 K show that there is good agreement between this work and the work of Brisley [7] in spite of the fact that a different electrolyte and reference materials were used. On increasing the temperature of the experiment it is found that from Tables 2–4 the dependence of the activity coefficient on the sodium concentration decreases as the temperature increases until at around 1068 K it is independent of the sodium content and the system obeys Henry's law; the values of the activity coefficients are similar to those given by Dewing [5] and derived from the phase diagram of Ransley and Neufeld [13]. This indicates that an association takes place between the sodium and the impurities, perhaps silicon, with aluminium at temperatures near to the melting point. There is a fair amount of scatter in the results and this is mainly due to difficulty of the sodium vaporization from the surface melt, its incorporation into the walls of the crucible and its subsequent release. Sodium oxide collects in the dross on the top of the aluminium bath and when the dross layer is disturbed, the sodium oxide reacts with the aluminium releasing sodium into the metal. There are, therefore, concentration profiles of sodium within the metal and it is scarcely surprising that the analytical results from a macrosample do not agree with the results given by the solid electrolyte probes. A similar scatter has been found when determining the oxygen content of steel using a stabilized zirconia probe [14, 15].

$Na_{0.75}CoO_2$ proved to have suitable properties as a reference powder. These are: (1) it is a good electronic conductor, (2) has a large range of homogeneity, (3) the partial molar-free energy of a sodium ion is constant over a wide range of composition, and (4) it appeared stable although there

Table 3. Activity coefficient of sodium in Al(99.5%) at 1068 K

ppm	$E_{(V)}$	a_{Na}	γ_{Na} This work	γ_{Na} Dewing (99.99% Al) [5]
1	1.03	4.29×10^{-4}	367	313
5	1.145	2.45×10^{-3}	256	313
10	1.22	3.38×10^{-3}	289	313
15	1.265	5.52×10^{-3}	313	313
20	1.285	6.86×10^{-3}	278	313

Table 4. Activity coefficient of sodium in Al(99.5%) at 1098 K

ppm	$E_{(V)}$	a_{Na}	γ_{Na} This work	γ_{Na} Dewing (99.99% Al) [5]
1	0.93	2.46×10^{-4}	210	290
5	1.08	1.202×10^{-3}	204	290
10	1.15	2.52×10^{-3}	215	290
15	1.195	4.06×10^{-3}	230	290
20	1.23	5.87×10^{-3}	237	290

was a slight interaction with the Nasicon tube whereas none was observed with the β-alumina tube.

5. Conclusions

A sodium probe based on Nasicon ($Na_3Zr_2Si_2PO_{12}$) and air-sintered $Na_{0.75}CoO_2$ solid solution electrode has been investigated and has been used to determine the activity of sodium in liquid aluminium. The results were in agreement with those of other workers at temperatures greater than 1068 K. Below 1068 K there appeared to be a strong interaction between impurities in the melt and the sodium leading to divergence from Henry's law.

The air-sintered $Na_{0.75}CoO_2$ solid solution proved to be a good sodium reference and its crystal structure was identified as the γ structure.

Acknowledgements

The authors are grateful for a studentship from the Chung Shan Institute of Science and Technology, Taiwan, Republic of China for P. C. Yao and to Alcan International Ltd, Arvida, Quebec for performing the analyses.

References

[1] R. C. Plumb and J. E. Lewis, *J. Inst. Metals* **86** (1957–58) 393.
[2] C. B. Kim and R. W. Heine, *ibid.* **92** (1963–64) 367.
[3] A. Hellawell, *Prog. Mater. Sci.* **15** (1970) 1.
[4] J. C. Mitchell and C. S. Samis, *Trans. TMS-AIME* **245** (1969) 1227.
[5] E. W. Dewing, *Metall. Trans.* **3** (1972) 495–501.
[6] D. J. Fray, *ibid.* **8B** (1976) 153.
[7] R. J. Brisley and D. J. Fray, *ibid.* **14B** (1983) 435.
[8] H. Y-P. Hong, *Mat. Res. Bull.* **11** (1976) 173.
[9] J. B. Goodenough, H. Y-P. Hong and J. A. Kafalas, *ibid.* **11** (1976) 203.
[10] B. C. H. Steele, 'Fast Ion Transport in Solids' edited by W. Van Gool, North Holland, Amsterdam (1973) p. 103.
[11] C. Fouassier, G. Matejka, J. M. Reau and P. Hagenmuller, *J. Solid State Chem.* **6** (1973) 532.
[12] C. Delmas, J. J. Braconnier, C. Fouassier and P. Hagenmuller, *Solid State Ionics* **3/4** (1981) 165.
[13] C. E. Ransley and H. Neufeld, *J. Inst. Metals* **78** (1950) 25.
[14] K. Yamada, Y. Shinya and K. Tanaka, *Solid State Ionics* **3/4** (1981) 595.
[15] M. Iwase and A. Maclean, in 'Fast Ionic Transport in Solids', edited by J. B. Bates and G. C. Farrington, North Holland, Amsterdam (198) pp. 571–74.
[16] R. J. Brisley, PhD Thesis, University of Cambridge, 1981.